CrystEngComm

Accepted Manuscript

This is an *Accepted Manuscript*, which has been through the Royal Society of Chemistry peer review process and has been accepted for publication.

Accepted Manuscripts are published online shortly after acceptance, before technical editing, formatting and proof reading. Using this free service, authors can make their results available to the community, in citable form, before we publish the edited article. We will replace this *Accepted Manuscript* with the edited and formatted *Advance Article* as soon as it is available.

You can find more information about *Accepted Manuscripts* in the Information for Authors.

Please note that technical editing may introduce minor changes to the text and/or graphics, which may alter content. The journal's standard Terms & Conditions and the Ethical guidelines still apply. In no event shall the Royal Society of Chemistry be held responsible for any errors or omissions in this *Accepted Manuscript* or any consequences arising from the use of any information it contains.

1   **Persistence of the self-complementary N-H⋯N tape motif in chloro-*s*-triazine crystals; crystal**

2   **structures of the simazine and atrazine herbicides, their polymorphic and inclusion behaviour.**

3

4   Thanh Le,[a] Mohan Bhadbhade,[b] Jiabin Gao,[b] James M Hook,[b] Christopher E Marjo[b,]*

5   [a] School of Chemistry, Chemical Sciences Building (F10), University of New South Wales, Kensington,

6   NSW, Australia 2052

7   [b] Mark Wainwright Analytical Centre, Room G61, Chemical Sciences Building (F10), University of New

8   South Wales, Kensington, NSW, Australia 2052

9

10   *Corresponding author. Tel.: +612 9385 9898; fax: +612 9385 4663.

11   E-mail address: c.marjo@unsw.edu.au

12   † Electronic supplementary information (ESI) available: crystal images and CIF files CCDC 1031279,

13   1031278, 1435451, 1435452.

14

15

16   **Abstract**

17   The *bis-N*-alkyl-chloro-*s*-triazines, simazine **1** and atrazine **2**, are potent and widely used commercial

18   herbicides; however, their crystal structures have been unreported to date. This study reports synchrotron

19   crystal structures of **1** and **2**, with the latter forming two polymorphs, as well as acting as a host structure

20   for three haloalkane guest molecules. The molecular assembly in all of the crystal structures is an N-H⋯N

21   hydrogen-bonded tape between hydrophobic phases formed by tightly packed alkyl side chains. The

22   hydrogen-bonded tape is persistent across all structures in this study, and a survey of the literature and the

23   Cambridge Structural Database (CSD) reveals the tape formation to be a persistent, highly stable motif in

24   a range of chloro-*s*-triazines. The tape morphology occurs as different sub-groups that correlate to the

25   volume of the *N*-substituent in a way that may permit a certain level of prediction and design for

26   unknown crystal structures.

27

28   **Introduction**

29   Hydrogen bonds are an important elements in the design of supramolecular structures,[1,2] and the

30   hydrogen-bonded tape is a common motif in the solid state with a history dating from the beginning of

31   supramolecular chemistry. There are numerous examples of co-crystals comprising tapes that form strong

32   NH⋯O hydrogen bonds[3,4] that can even persist when one of the hydrogen bonding interactions is

33   "deleted" for example when a chlorine atom is present in the triazine[5]. Other tape interactions include

34   OH⋯O hydrogen bonding in dicarboxylic acids,[6] and weaker hydrogen bonds (CH⋯N) that form

35   persistent tapes in the solid state.[7] Nitrogen-containing heteroaromatic amines can be engineered to

36   produce self-complementary NH···N hydrogen-bonded tapes,[8,9] and the amino-triazines and amino-

37   pyrimidine systems are particularly effective.[10,11] The robustness of hydrogen-bonded tapes makes them a

38   reliable synthon for design in the solid state where they may persist in the presence of other non-covalent

39   interactions. There are numerous examples of current studies where hydrogen-bonded tapes continue to

40   be effective tools for crystal engineering.[12,13,14,15,16]

41

42   This study describes the solid state behaviour of a range of *bis*-*N*-dialkyl-chloro-*s*-triazines, particularly

43   simazine, 6-chloro-2-*N*,4-*N*-diethyl-1,3,5-triazine-2,4-diamine **1**, and atrazine, 6-chloro-4-*N*-ethyl-2-*N*-

44   propan-2-yl-1,3,5-triazine-2,4-diamine **2** (Figure 1). These compounds have an ideal configuration of

45   hydrogen bond donors and acceptors to permit infinite self-complementary interactions in the solid state.

46   Compounds **1** and **2** have been used for many decades as selective systemic herbicides worldwide,[17,18] and

47   **2** was the second most common herbicide in the United States after glyphosate in 2007, with an estimated

48   33-35 million kg applied to crops.[19] The biological function of these herbicides is to inhibit the selective

49   binding of plastoquinone (PQ) in the chloroplast of the plant interrupting photosynthetic electron transfer,

50   thus compromising ATP energy production and NADPH synthesis causing oxidative stress and rapid

51   cellular damage. Crystallographic studies on the binding of atrazine to the reaction centre of

52   rhodopseudomonas viridis[20] and glutathione-S-transferase[21] have been reported; however, the structures

53   of the pure herbicide molecules **1** and **2** have not been determined, probably due to their tendency to form

54   microcrystals only a few tens of micrometres in width that are unsuitable for standard crystallographic

55   analysis.

56
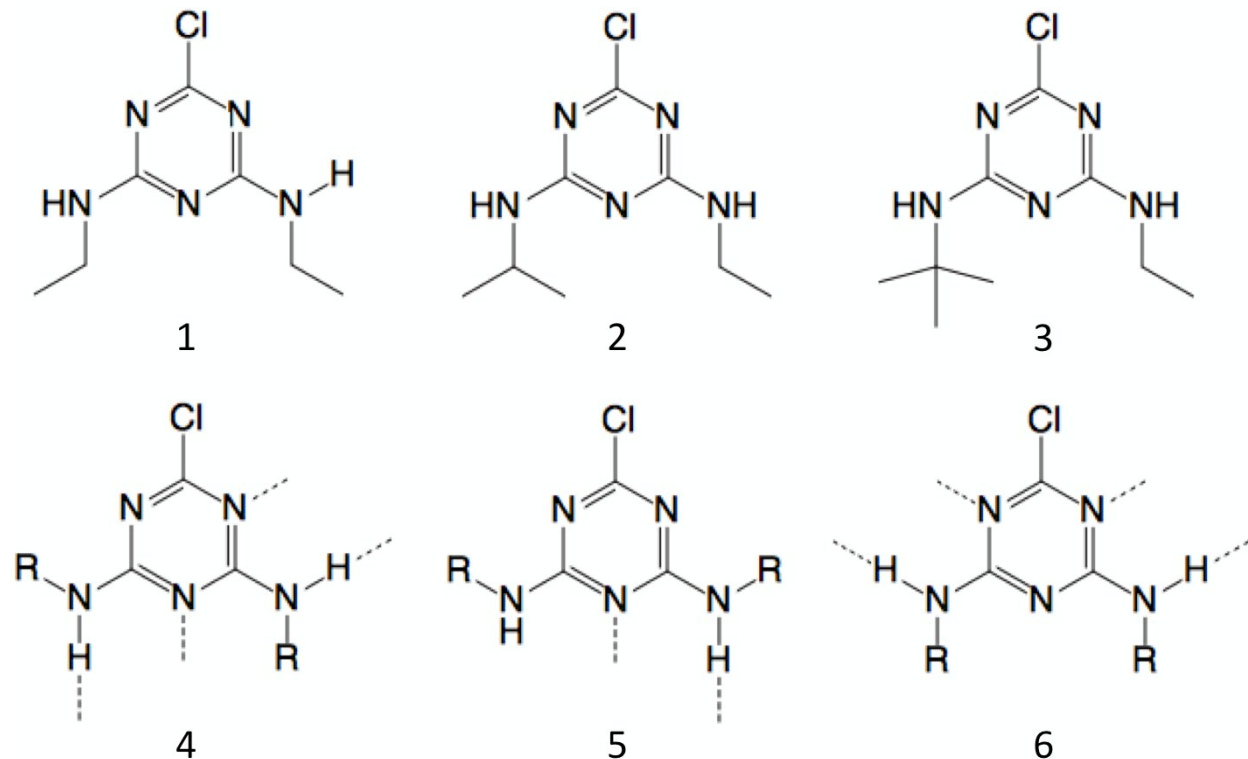
Figure 1: Compounds **1**, **2** and **3**, *s*-triazines investigated in this study, and **4**, **5**, and **6**, potential conformers of this class of *N*-alkyl-*s*-triazine.

Amino groups on heteroaromatic rings are well known to have amide-like character,[22] where the nitrogen lone-pair is delocalised into the ring and the substituents are planar, tending to lie parallel to the aromatic ring. The energy barrier for rotation about the aromatic C-N bond results in three potential *cis* and *trans* conformers shown in Figure 1, **4**, **5** and **6** (or four if the R groups differ on the molecule). However, only conformer **6** has been reported in the crystal structure of the related herbicide, terbuthylazine **3**, and a range of other chloro-*s*-triazines.[23] Conformer **5** has alkyl groups blocking two edges from self-complementary hydrogen bonding, while **4** and **6** has its alkyl groups oriented to expose two edges, thus maximising the number of hydrogen bonds (broken lines in Figure 1) in the solid state. Conformer **4** is not observed in the solid state in **1**, **2** or **3**, presumably due to the unfavourable interaction between two R-groups required for self-complementary interaction on the lower edge of the molecule.

In this study we report for the first time the crystal structures of **1** and **2** solved using a high intensity X-ray source at the Australian Synchrotron. We confirm that both compounds are hydrogen-bonded tape-formers, and we note the ubiquity of this tape motif, observing it in the crystal structures of atrazine

75   polymorphs, atrazine inclusion complexes, and in related chloro-*s*-triazines in the literature. Examination

76   of crystal structures formed by **1**, **2** and **3** illustrates the influence of increasing substituent size on the tape

77   morphology. The inclusion behaviour of **1**, **2** and **3** was also investigated using a range of common

78   solvents, with three inclusion compounds observed for **2**. A comprehensive search of chloro-*s*-triazines in

79   the CSD shows that the tape persists in chloro-*s*-triazines substituted with a diverse range of *N*-alkyl

80   groups. The tape can adopt a range of morphologies, yet still produce the self-complementary edge-edge

81   interaction with the expected N⋯N distances from a normal hydrogen bond. The contortions of the tape

82   are not continuous, but can be categorised within a limited angular range that correlates with the shape

83   and volume of the *N*-alkyl groups.

84

85   **Results and Discussion**

86   Crystallographic analysis of simazine **1** and atrazine **2** prepared from a range of solvents produced a

87   single crystalline form **1**$_{Form\_I}$, two polymorphs **2**$_{Form\_I}$ and **2**$_{Form\_II}$, and three unstable inclusion complexes

88   from chloroform, **2**.**CHCl$_3$**, bromoform, **2**.**CHBr$_3$**, and 1,1,2,2-tetrachloroethane, **2**.**TCE**. Tests for

89   inclusion compounds of terbuthylazine **3** produced only the previously reported crystalline form.[23] Of the

90   three inclusion complexes, only **2**.**TCE** produced acceptable structural data. Table 1 gives the parameters

91   of the solution and refinement of the four well-refined crystal structures reported in this study. The

92   crystals of **2**$_{Form\_I}$ were very thin needles, and the crystals of **2**.**TCE** inclusion complex exhibited only

93   weak diffraction. Both crystals revealed different orientational disorders that would affect the diffraction

94   profiles of high angle reflections. As a consequence of weak diffraction and disorder **2**$_{Form\_I}$ and **2**.**TCE**

95   produced relatively higher R_{int} and weighted R values (wR) than were observed for **1**$_{Form\_I}$ and **2**$_{Form\_I}$.

96

97   Figure 2 shows the ORTEP diagrams and for the crystal structures reported here. The *N*-alkyl

98   conformation in all four of the crystal structures leaves no doubt as to the preferred orientation imposed

99   by the solid state. Despite variations in the size and substitution of the alkyl group, it is always positioned

100   to expose two edges of the molecule to self-complementary N-H⋯N hydrogen bond interaction. This

101   conformation is favoured, despite resulting in unfavourable steric interaction between the *N*-alkyl groups,

102   that tend to be rotated orthogonal to the plane of the triazine ring to minimise this interaction.

103

104

(a)   (b)

(c)   (d)
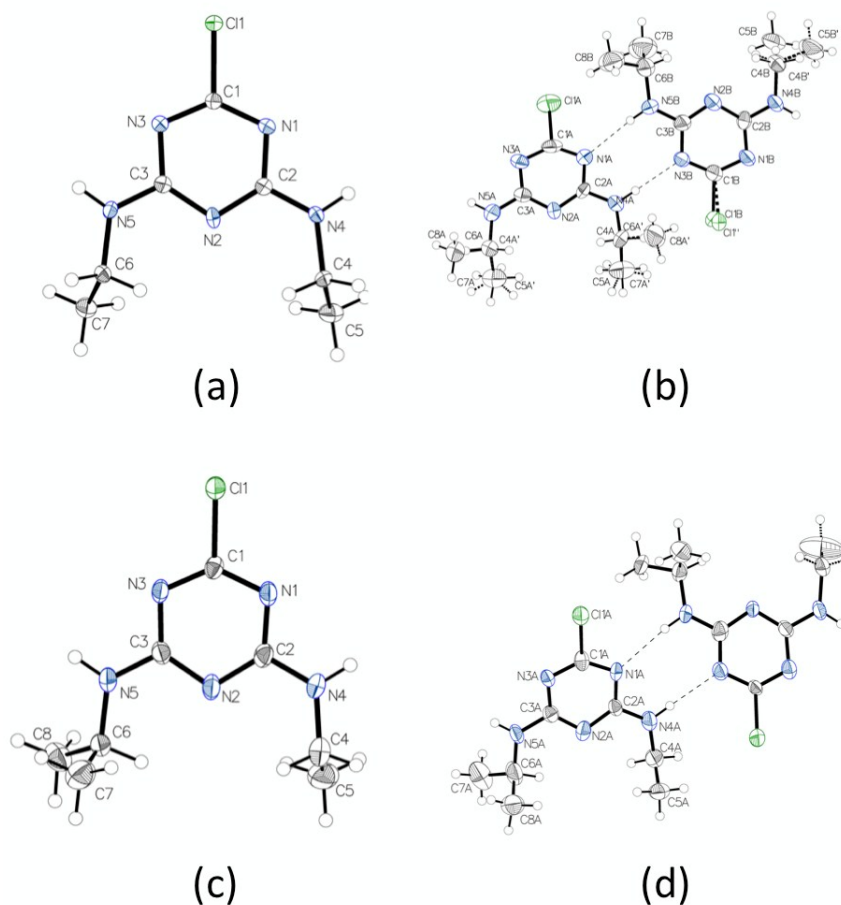
Figure 2: Asymmetric unit (AU) of the crystal structures reported in this study: (a) Simazine 1_{Form_I} ORTEP; (b) Atrazine 2_{Form_I} ORTEP of two molecules in the AU; (c) Atrazine 2_{Form_II} ORTEP; and (d) ORTEP of **2.TCE**, with the guest removed for clarity. ORTEP structures are displayed with atom labelling and ellipsoids drawn at 50% probability level.

Table 1: Numerical details of the solution and refinement of the crystal structures

Compound	1_{Form_I}	2_{Form_I}	2_{Form_II}	**2.TCE**
CCDC Deposition Number	1031279	1031278	1435451	1435452
Formula	$C_7H_{12}ClN_5$	$C_8H_{14}ClN_5$	$2(C_8H_{14}ClN_5)$	$2(C_8H_{14}ClN_5)\cdot 2(C_2H_2Cl_4)$
Formula mass	201.67	215.69	431.38	767.05

Crystal system	Monoclinic	Orthorhombic	Orthorhombic	Monoclinic
Space group	$P2_1/c$	$Fdd2$	$Pbca$	$P2_1/c$
Temperature (K)	100	150	100	150
a	4.4390 (9)	34.2012 (19)	19.847 (4)	11.908 (3)
b	11.980 (2)	10.3247 (6)	9.6160 (19)	19.374 (7)
c (Å)	17.852 (4)	12.1234 (6)	23.793 (5)	15.441 (5)
β (°)	94.04 (3)			105.86 (2)
V (Å^3)	947.0 (3)	4281.0 (4)	4540.9 (16)	3426.7 (18)
Z	4	16	8	4
μ (mm^{-1})	0.37	0.33	0.31	0.84
Crystal size (mm)	0.02 × 0.02 × 0.02	0.25 × 0.06 × 0.04	0.02 × 0.01 × 0.01	0.30 × 0.14 × 0.04
T_{min}, T_{max}	0.993, 0.995	0.977, 0.986	0.996, 0.997	0.872, 0.971
No. of measured, independent, and observed [$I > 2\sigma(I)$] reflections	11556, 1600, 1495	13347, 1786, 1629	34417, 2548, 1657	29898, 7503, 2370
R_{int}	0.038	0.033	0.157	0.226
$(\sin\,\theta/\lambda)_{max}$ (Å^{-1})	0.594	0.594	0.512	0.642
R [$F^2 >$	0.044	0.044	0.110	0.091

$2\sigma(F^2)$]				
w$R(F^2)$	0.131	0.118	0.256	0.301
S	1.02	1.04	1.14	0.97
No. of reflections	1600	1786	2548	7503
No. of parameters	120	130	299	425
No. of restraints	—	1	46	103
$\Delta>_{max}$, $\Delta>_{min}$ (e Å^{-3})	0.85, -0.30	0.48, -0.21	0.28, −0.28	0.71, −0.42
Abs. struct. parameter	—	0.69 (2)	—	—
CSD reference code	PORJOX	PORJIR	—	—

112

113

(a)

(b)   (c)

(d)   (e)
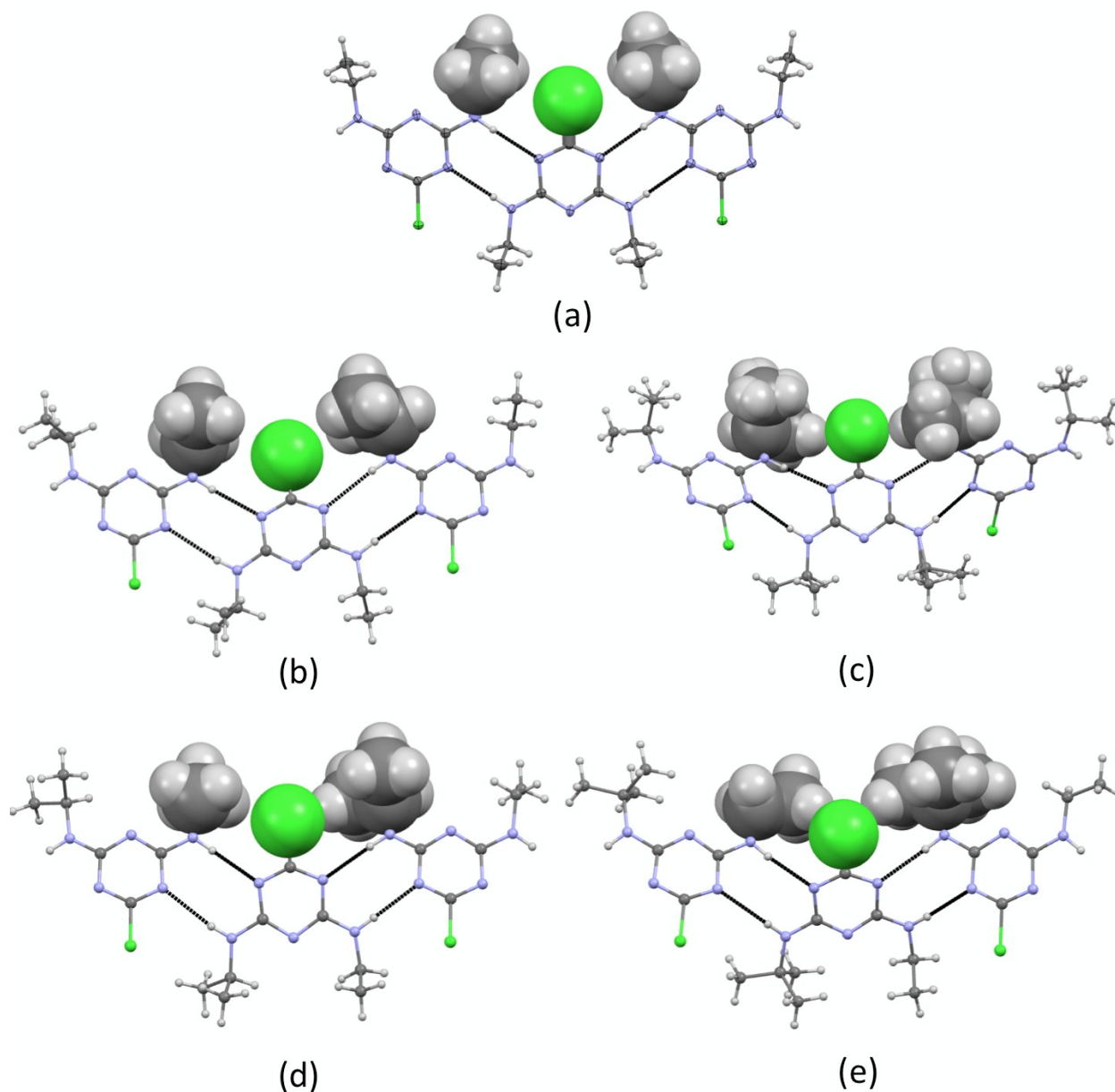
114

115   Figure 3: Portions of hydrogen-bonded tapes found in the crystal structure of (a) 1_{Form_I}, the polymorphs

116   (b) 2_{Form_I}, (c) 2_{Form_II}, (d) the inclusion complex $2 \cdot \text{TCE}$ (only two chains shown for clarity), and (e) the

117   previously reported structure for terbuthylazine 3.[23] A selection of alkyl side chains and chlorine atoms

118   are rendered using space filling to visualise VDW packing.

119

120   In all five structures, the consistent feature is an infinite one-dimensional hydrogen-bonded molecular

121   tape. A selected portion of the infinite one-dimensional tape in 1_{Form_I}, 2_{Form_I}, 2_{Form_II}, $2 \cdot \text{TCE}$, and 3 is

122   shown in Figure 3. The tapes define a polar hydrogen-bonded phase in each crystal surrounded by close-

123   packed hydrophobic phase of *N*-alkyl groups. Each triazine edge-to-edge interaction in the tape defines a

124 dimeric N-H···N interaction that is self-complementary with respect to each hydrogen bond, although not

125 with respect to the crystal structure. Despite the similar features, there are obvious differences

126 necessitated by the changing volume and shape of the *N*-alkyl group. In simazine 1_{Form_I} with a single

127 molecule in the asymmetric unit, the N-H···N association along the infinite one-dimensional tape is

128 generated along the 2_1 screw axis (along the b-axis). Interestingly, the atrazine 2_{Form_I} also contains tapes

129 along the 2_1 screw axis (b-axis), although the space group is orthorhombic *Fdd*2. The atrazine 2_{Form_II} and

130 **2.TCE** inclusion compound both contain two molecules in the asymmetric unit, which are associated via

131 N-H···N bonds. These dimeric units are buckled with an angle between the planes of the aromatic rings of

132 34 º in 2_{Form_II} and 28 º in **2.TCE**. The tapes in these cases are formed by a c-glide symmetry operator in

133 2_{Form_II} and by unit translation along the c- axis in **2.TCE**. Atrazine 2_{Form_II} and terbuthylazine **3** belong to

134 the same crystal system (orthorhombic), but the former has a centrosymmetric space group symmetry

135 *Pbca*, whereas the latter is in non-centrosymmetric *Pca*2(1). There are only two molecules in the

136 asymmetric unit (blue and green) of Atrazine 2_{Form_II}, whereas there are four molecules (yellow, green

137 and red, blue) in crystals of terbuthylazine. The centrosymmetry is created only statistically because of

138 the two-fold orientational disorder in blue molecules that creates the equivalence across (red) centres of

139 inversion. There is no such disorder exhibited by the molecules of terbuthylazine in its crystal form

140 (supplementary Figure S4).

141

142 The tapes seen in 1_{Form_I} and 2_{Form_I} are similar in the sense that the hydrogen-bonded triazine rings lie in

143 the same plane. The geometrical parameters for the strong hydrogen bonds (Table 2) show the variations

144 in N-H···N contacts in these structures. The atrazine 2_{Form_I} has one N-H···N contact somewhat longer (N5-

145 H5···N1 = 3.216 Å) compared to other N-H···N distances, but the molecule appears to compensate with a

146 shorter C-H···Cl distance (~2.88 Å) when compared to 1_{Form_I}. The tapes in atrazine 2_{Form_II} and the

147 atrazine **2.TCE** inclusion complex are both non-planar compared to 1_{Form_I}. Of these two structures, the

148 tape in 2_{Form_II} shows more buckling than the tape in **2.TCE**, with a side-chain disorder slightly above and

149 below the plane to ensure close packing. In the **2.TCE** inclusion structure, both of the side chains and the

150 TCE guest are involved in close C-H···Cl contacts in the close-packed hydrophobic region where the side-

151 chain is immobilised. The side chain interactions between tapes 1_{Form_I}, 2_{Form_I}, 2_{Form_II}, and **2.TCE** are

152 shown in Figures S1 and S2 (supplementary information). Interactions between the triazine rings in 1_{Form_I}

153 and 2_{Form_I} are displayed in Figure S3 (supplementary information).

154

155 The self-complementarity of the chloro-*s*-triazine structure places more restrictions on the tape than other

156 systems explored in the literature. One of the most thoroughly investigated of these is the melamine-

157 barbiturate hydrogen-bonded tape reported by the group of Whitesides, where the two components were

158   designed to form DAD-ADA hydrogen bond interactions (D = NH donor, A = N/O acceptor) regardless

159   of their relative orientation.[3,4,5] As a result of this flexibility a wide variety of melamine-barbiturate

160   crystals were observed forming linear or "crinkled" tapes, or the cyclic "rosette" structure in the solid

161   state, depending on the size of the melamine *N*-substituent. By comparison the chloro-*s*-triazine

162   molecules in this study are limited to a self-complementary two hydrogen bond DA-AD interaction to

163   form tapes, and the crinkled and cyclic rosette forms are not possible. An advantage of this restriction is

164   that tape morphology in this series is easier to classify, as the most significant difference is described by

165   the angle formed between the plane passing through adjacent triazine rings, although there may be up to

166   three interplanar angles in low symmetry structures such as 2_{Form_II}.

167

168   The least complex tape is that found in simazine 1_{Form_I} (Figure 3a) where there is essentially no deviation;

169   the triazine rings lie in the same plane, a morphology we designate as "linear". The next level of tape

170   complexity we designate as "buckled" is the tape found in atrazine 2_{Form_I} that shows a slight modulation

171   from planarity (Figure 3b) and makes C-Cl···C-Cl centrosymmetric dipolar contacts between chains

172   (supporting data Figure S1). The polymorph atrazine 2_{Form_II} (Figure 3c) shows considerable deviation

173   from planarity as does its inclusion complex with TCE (Figure 3d), and the less well-refined $CHCl_3$ and

174   $CHBr_3$ inclusion structures suggest this as well (not shown). This more distorted tape we designate as

175   "twisted". Inclusion of haloalkane solvents provides one solution to the problem of producing a close-

176   packed structure from these mismatched *N*-ethyl and *N*-isopropyl groups in **2**. Inclusion of solvent

177   molecules, as well as polymorphism, was a notable characteristic of the stable melamine-barbiturate tapes

178   explored by Whitesides.[4] The homologous terbuthylazine **3** (Figure 3e) is still able to solve the close-

179   packing of its bulky *N*-*t*-butyl groups, and does so with a similar degree of tape buckling as that found in

180   the three atrazine structures.

181

182   A search of the Cambridge Structural Database (CSD) for chloro-s-triazines substituted with two RNH

183   groups, and no geometrical constraints, produced 28 results that included the recently deposited 1_{Form_I}

184   and 2_{Form_I}. Each of the 28 structures was assessed manually to identify N-H···N hydrogen bonds (N···N

185   distance < 3.5 Å, N-H···N angle > 120 º) between edges of adjacent molecules. The planes of the triazine

186   rings were observed to intersect at an angle < 70 º. The search revealed the self-complementary N-H···N

187   hydrogen bond was present in 6 other members of the chloro-*s*-triazine family (Table 3), in addition to the

188   structures already discussed. The self-complementary tape will form whenever the *N*-substituents can

189   expose both triazine edges to hydrogen bonding, and the VDW packing problem between the tapes can be

190   "solved" to produce a hydrophobic domain parallel to the hydrogen bonds.[31] When an additional

191   hydrogen bond acceptor (N or O) is present in other parts of the *N*-substituent or an included guest

192   molecule (such as THF or DMSO), tape formation can be disrupted or prevented entirely. However, we

193   note that acetone inclusion is an exception to this, still permitting tape formation despite contributing a

194   hydrogen bond acceptor. Despite these exceptions, the dominance of this tape motif that suggests that it

195   may persist across a large range of chloro-*s*-triazines yet to be analysed or synthesized.

196

197   **Table 2 N-H···N hydrogen bond geometry parameters.**

198   **1**$_{Form\_I}$, Hydrogen-bond geometry (Å, º)

D—H···A	D—H	H···A	D···A	D—H···A
N4—H4···N3[i]	0.88	2.17	3.043 (2)	174
N5—H5···N1[ii]	0.88	2.19	3.051 (2)	167

199   Symmetry codes: (i) −*x*+2, *y*+1/2, −*z*+3/2; (ii) −*x*+2, *y*−1/2, −*z*+3/2;

200

201   **2**$_{Form\_I}$, Hydrogen-bond geometry (Å, º)

D—H···A	D—H	H···A	D···A	D—H···A
N4—H4···N3[i]	0.88	2.19	3.061 (6)	173
N5—H5···N1[ii]	0.88	2.36	3.216 (6)	163

202   Symmetry codes: (i) −*x*+2, −*y*+3/2, *z*+1/2; (ii) −*x*+2, −*y*+3/2, *z*−1/2;

203

204   **2**$_{Form\_II}$, Hydrogen-bond geometry (Å, º)

D—H···A	D—H	H···A	D···A	D—H···A
N4*B*—H4*B*···N3*A*[i]	0.88	2.14	2.999 (11)	165
N5*B*—H5*B*···N1*A*	0.88	2.18	3.055 (11)	175
N4*A*—H4*AA*···N3*B*	0.88	2.16	3.039 (11)	174
N5*A*—H5*AA*···N1*B*[ii]	0.88	2.18	3.058 (11)	175

205   Symmetry codes: (i) *x*, −*y*+3/2, *z*+1/2; (ii) *x*, −*y*+3/2, *z*−1/2;
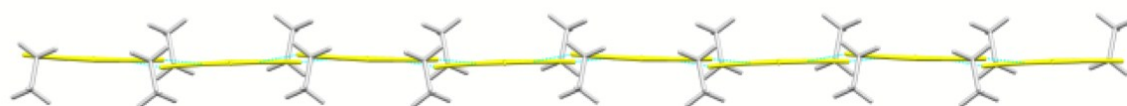
206

207   **2.TCE**, Hydrogen-bond geometry (Å, º)

D—H···A	D—H	H···A	D···A	D—H···A
N4*B*—H4*B*···N3*A*[i]	0.88	2.20	3.068 (9)	169
N5*B*—H5*B*···N1*A*[ii]	0.88	2.27	3.140 (8)	171
N4*A*—H4*A*···N3*B*[iii]	0.88	2.11	2.985 (9)	175

| N5A—H5A···N1Biv | 0.88 | 2.32 | 3.193 (9) | 171 |

208 Symmetry codes: (i) *x*+1, −*y*+3/2, *z*+1/2; (ii) *x*, −*y*+3/2, *z*+1/2; (iii) *x*, −*y*+3/2, *z*−1/2;

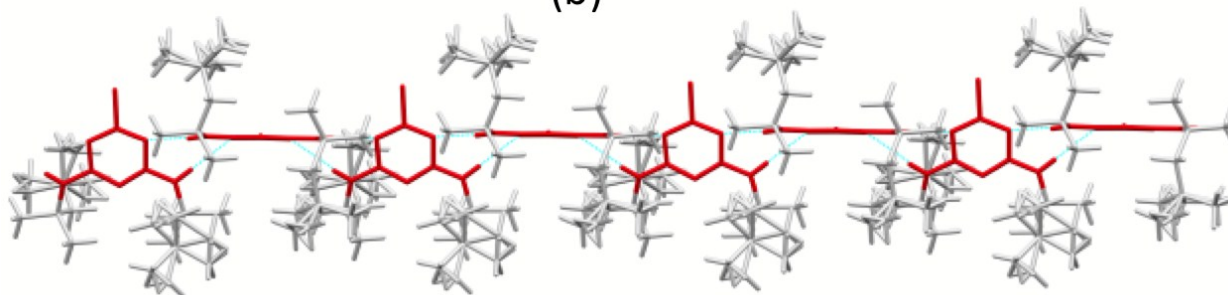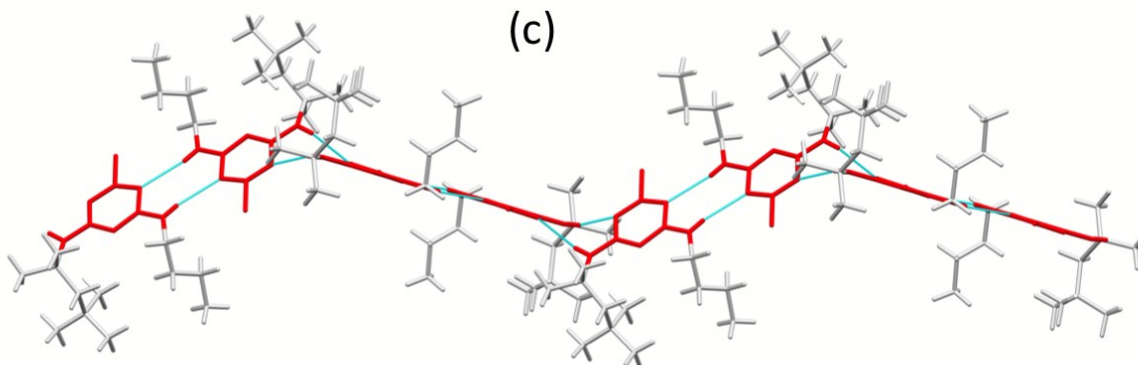209 (iv) *x*−1, −*y*+3/2, *z*−1/2
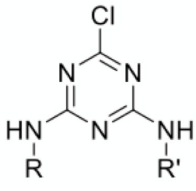
210

(a)
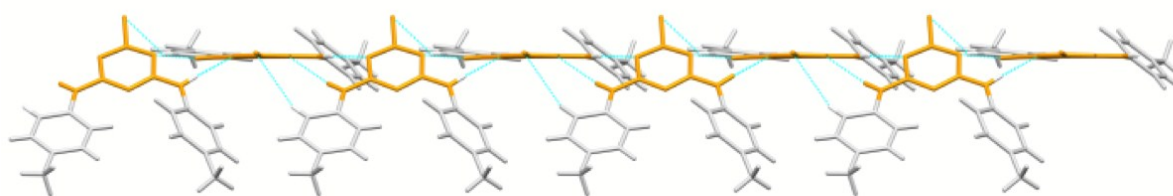
(b)

(c)

(d)

211
212 Figure 4: Examples of the four N-H···N tape morphologies found in the CSD: (a) linear tape in simazine
213 **1**Form_I, (b) buckled tape in NIQWAM, (c) twisted tapes in UDUVEV, and (d) the zigzag tape in

214   WIHHEB, a hybrid of the linear and twisted forms. The chloro-*s*-triazine moieties are coloured to

215   represent their respective interplanar angle groups shown in Figure 5 with the substituents shown in grey.

216

217   Figure 4 shows four examples from the CSD search that are representative of our three tape

218   morphologies. The simazine 1_{Form_I} is an ideal linear example with its small *N*-ethyl substituents (Figure

219   4a). Replacement with larger *p*-tolyl substituents in NIQWAM (Figure 4b) produces a buckled tape with

220   acetone inclusion, while large alkyl groups with a number of tertiary-substituted carbon atoms produces

221   the twisted variety found in UDUVEV (Figure 4c). Interestingly, reducing the size of one of the

222   substituents to *n*-propyl in WIHHEB produces the zigzag sub-class (Figure 4d), a composite of linear

223   "dimers" that associate via the bent hydrogen bonds found in the buckled form. The data from the CSD

224   search for *N*-substituent volume and triazine interplanar angles is given in Table 3.

225

226   Table 3. chloro-*s*-triazines from the CSD observed to form the N-H⋯N tape motif.

Structure, and/or CSD Ref.	R Vol.(Å^3)	R' Vol.(Å^3)[30]	Guest Vol.[30] (Å^3)	Total Vol. (Å^3)	Interplanar angles (°)		
1_{Form_I} PORJOX	-CH$_2$CH$_3$ 46	-CH$_2$CH$_3$ 46	—	92	4	—	—
2_{Form_I} PORJIR	-CH$_2$CH$_3$ 46	-CH(CH$_3$)$_2$ 66	—	112	14	—	—
2_{Form_II}	-CH$_2$CH$_3$ 46	-CH(CH$_3$)$_2$ 66	—	112	43	29	—
2.TCE	-CH$_2$CH$_3$ 46	-CH(CH$_3$)$_2$ 66	(CHCl$_2$)$_2$ 168	112	29	—	—
3	-CH$_2$CH$_3$	-C(CH$_3$)$_3$	—	125	41	41	—

JODMOF	46	79					
WIHHEB	-CH$_2$CH$_2$CH$_3$ 63	-C(CH$_3$)$_2$CH$_2$C(CH$_3$)$_3$ 146	—	208	64	0	—
DOBCAA	-CH$_2$COOCH$_3$ 74	-CH$_2$COOCH$_3$ 74	—	147	0	—	—
UFAGUE	-(CH$_2$)$_3$CH$_3$ 79	-C(CH$_3$)$_2$CH$_2$C(CH$_3$)$_3$ 146	—	225	61	0	—
NIQWAM	-*p*-tolyl 101	-*p*-tolyl 101	CH$_3$COCH$_3$ 65	202	47	—	—
SILPEJ	-benzyl 101	-C(CH$_3$)$_2$CH$_2$C(CH$_3$)$_3$ 146	—	246	59	61	0
UDUVEV	-C(CH$_3$)$_2$CH$_2$C(CH$_3$)$_3$ 146	-C(CH$_3$)$_2$CH$_2$C(CH$_3$)$_3$ 146	—	291	62	—	—

227
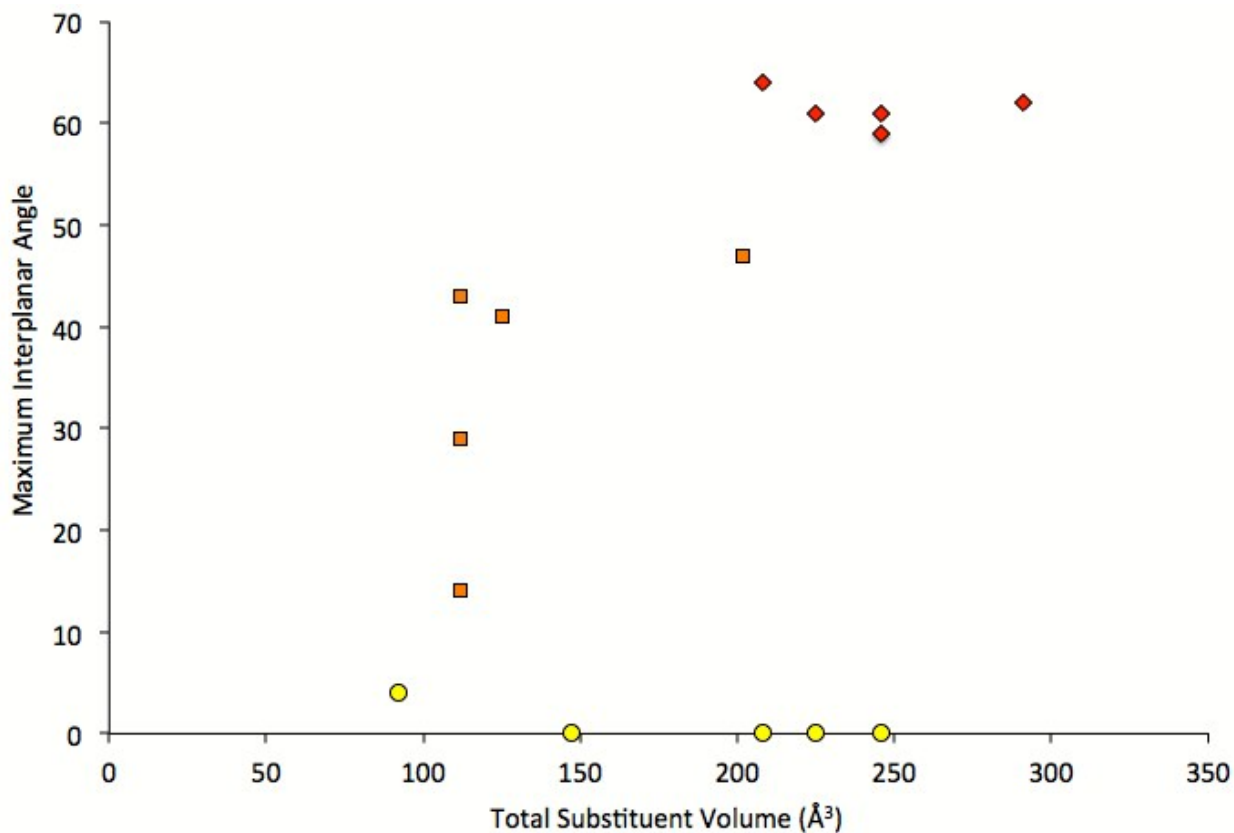
228

229   Figure 5. Interplanar angle vs. total substituent volume of chloro-*s*-triazines structures in N-H$\cdots$N tapes

230   found in the CSD. The interplanar angles have been grouped into three categories: linear (0-10º, yellow

231   circles), buckled (10-50°, orange squares), and twisted (50-70°, red diamonds).

232

233   Figure 5 is a plot of all interplanar angles observed between triazines against the total volume of the *N*-

234   substituents in each structure in the CSD search. Triazine interactions in the tapes are arbitrarily grouped

235   into linear (0-10°, yellow circles), buckled (10-50°, orange squares), and twisted geometries (50-70°, red

236   diamonds). A single structure may display multiple geometries, as in WIHHEB in Figure 4d that is

237   actually a hybrid of the linear and twisted forms. Substituent shape clearly plays a role as a wide range of

238   substituent volumes can maintain the linear interaction. However, for many substituents there is a positive

239   correlation with increasing substituent volume and distortion of the tape to accommodate these larger

240   substituents. While not completely predictive this relationship persists across a range of space groups and

241   in the presence of included guest molecules, and should act as a guiding principle for future crystal

242   engineering in these structures.

243

244   The relationship between *N*-substituent and chain morphology suggests that the chain morphology of

245   novel chloro-*s*-triazines, or chloro-*s*-triazines with unknown crystal structures could be predicted. The

246   persistence of the tape suggests it could be used for pre-organisation for solid-state reactions between

247   appropriately functionalised adjacent *N*-substituents. For example, chloro-*s*-triazines *N*-substituted with

248   linear chains such as *n*-propyl, *n*-butyl, *n*-pentyl etc. should crystallise in a structure analogous to that of

249   the *N*-ethyl, **1**$_{Form\_I}$, with neighbouring chains aligned in the crystal structure. Incorporation of double

250   bonds in the chain may enable an X-ray induced topotactic polymerisation or dimerisation within the

251   crystal in high yield.[32,33] Alternatively chiral amino esters may induce chiral-secondary structure into solid

252   state tapes.

253

254   **Experimental**

255   **Materials**: Technical grade samples of **1**, **2**, and **3** were used for crystallisation without any further

256   purification. Solvents used for the crystallisation experiments were purchased from Sigma-Aldrich or

257   Alfa-Aesar and used as received.

258   **Simazine 1**$_{Form\_I}$ was found to crystallise from solutions of **1** in ethanol, methanol, dichloromethane,

259   chloroform, bromoform, 1,1,2,2-tetrachloroethane, dimethyl sulfoxide, dimethylformamide and acetone.

260   Only a single crystalline form was produced from these solvents, and fine-needles produced from ethanol

261   were used for subsequent crystallographic analysis.

262   **Atrazine 2**$_{Form\_I}$ was found to crystallise from hot solutions of **2** in anhydrous ethanol, dimethyl sulfoxide,

263   dimethylformamide, nitromethane, or acetone. Fine needles suitable for synchrotron crystallographic

264   analysis were produced by dissolving in hot anhydrous ethanol then allowing the crystals to form slowly

265   on cooling to room temperature.

266   **Atrazine 2**$_{Form\_II}$ was obtained by dissolving **2**$_{Form\_I}$ in hot ethanol (95%), then adding the same volume of

267   water dropwise with stirring to ensure a clear solution, then allowing crystals to form slowly at room

268   temperature.

269   **Atrazine 2**.**TCE**, the inclusion complex of **2** with 1,1,2,2-tetrachloroethane, were grown *via* slow

270   evaporation of a concentrated solution of **2** in 1,1,2,2-tetrachloroethane to produce crystals that were

271   protected in paraffin, suitable for synchrotron crystallographic analysis.

272   Inclusion complexes of atrazine, **2.CHCl₃** and **2.CHBr₃** grown by rapid evaporation from solution;

273   however, rapid desolvation of these complexes compromised the data available from synchrotron analysis

274   despite efforts to preserve the crystals in paraffin.

275   **Terbuthylazine 3** was tested for inclusion behaviour by crystallising from methanol, ethanol, chloroform

276   and bromoform; however, in all these cases **3** was found to crystallise as the previously reported **3**$_{Form\_I}$.[23]

277   **Laboratory-based single crystal X-ray analysis**: suitable single crystals of **2**$_{Form\_I}$ and **2.TCE** were

278   selected under the polarizing microscope (Leica M165Z), mounted on a MicroMount (MiTeGen, USA)

279   consisting of a thin polymer tip with a wicking aperture. The X-ray diffraction measurements were carried

280   out on a Bruker kappa-II CSD diffractometer at 150 K by using IμS Incoatec Microfocus Source with

281   Mo-Kα radiation (λ = 0.710723 Å). The single crystal, mounted on the goniometer using cryo loops for

282   intensity measurements, was coated with paraffin oil and then quickly transferred to the cold stream using

283   an Oxford Cryostream attachment. Symmetry related absorption corrections using the program

284   SADABS[24] were applied and the data were corrected for Lorentz and polarisation effects using Bruker

285   APEX2 software.[25] The structure was solved by direct methods and the full-matrix least-square

286   refinement was carried out using SHELXL[26] in Olex2.[27] The non-hydrogen atoms were refined

287   anisotropically. The molecular graphics were generated using Olex2[27] and Mercury (2015 CSD

288   Release).[28]

289   **Synchrotron-based single crystal X-ray analysis**: the X-ray diffraction measurements for 1_{Form_I},

290   2_{Form_II}, and 3_{Form_I} were carried out on the MX1/ MX2 beamline at the Australian Synchrotron Facility,

291   Melbourne. The crystal was mounted on the goniometer using a cryo loop for diffraction measurements,

292   was coated with paraffin oil and then quickly transferred to the cold stream using the Cryo stream

293   attachment. Data were collected using Si<111> monochromated synchrotron X-ray radiation (λ = 0.71023

294   Å) at 100(2) K and were corrected for Lorentz and polarization effects using the XDS software.[29] The

295   structure was solved by direct methods and the full-matrix least-squares refinements were carried out

296   using SHELXL[26] and with Olex-2.[27]

297   **Molecular volume** calculations on *N*-substituents were performed using the Molinspiration Property

298   Calculation Service (www.molinspiration.com).[30]

299   **Cambridge crystallographic database analysis** was performed using ConQuest[28] (2015 CSD Release)

300   to search for crystal structures of di-(*N*-alkylamine)-chloro-*s*-triazines where the alkyl group was

301   unconstrained. The resulting structures were visualised to look for self-complementary tapes, then the

302   tapes evaluated by measuring the inter-planar angles between each triazine ring as a parameter for

303   classifying different tape morphologies.

304

305   **Conclusion**

306   Synchrotron crystal structures of the herbicides simazine **1** and atrazine **2** are reported for the first time,

307   and polymorphism and solvent inclusion are observed for atrazine. The self-complementary hydrogen

308   bonds enable tape formation in the solid state, and this tape motif is observed in all structures reported in

309   this study and in numerous related chloro-*s*-triazines in the literature. Increasing substituent size is

310   observed to produce three distinct types of tape morphology, and a correlation with the volume of the *N*-

311   substituent group is observed. This correlation suggests that the tape morphology may be open to control

312   by selection of the appropriate *N*-substituent in novel or structurally uncharacterised chloro-*s*-triazine

313   compounds.

319   **References**

320   1. M. C. Etter, *J. Phys. Chem.*, 1991, **95**, 4601.

321   2. C. B. Aakeröy and A. M. Beatty, *Aust. J. Chem.*, 2001, **54**, 409.

322   3. J. A. Zerkowski, J. P. Mathias and G. M. Whitesides, *J. Am. Chem. Soc.*, 1994, **116**, 4305.

323   4. J. A. Zerkowski and G. M. Whitesides, *J. Am. Chem. Soc.*,1994, **116**, 4298.

324   5. J.A. Zerkowski, J. C. MacDonald and G. M. Whitesides, *Chem. Mater.*, 1994, **6**, 1250.

325   6. J. C. MacDonald and G. M. Whitesides, *Chem. Rev.*, 1994, **94**, 2383.

326   7. R. Bishop, C. E. Marjo and M. L. Scudder, *Mol. Cryst. Liq. Cryst.*, 1998, **313**, 75.

327   8. A. Duong, T. Maris and J. D. Wuest, *Cryst. Growth Des.*, 2010, **11**, 287.

328   9. A. Duong, T. Maris, O. Lebel and J. D. Wuest, *J. Org. Chem.*, 2011, **76**, 1333.

329   10. S. Mahapatra, S. K. Nayak, S. J. Prathapa and T. N. Guru Row, *Cryst. Growth Des.*, 2008, **8**, 1223.

330   11. P. Li, H. D. Arman, H. Wang, L. Weng, K. Alfooty, R. F. Angawi and B. Chen., *Cryst. Growth Des.*,

331   2015, **15**, 1871.

332   12. R. Takasawa, I. Yoshikawa and K. Araki, *Org. Biomol. Chem.*, 2004, **2**, 1125.

333   13. S. K. Sommer, L. N. Zakharov and M. D. Pluth, *Inorg. Chem.*, 2015, **54**, 1912.

334   14. V. G. Saraswatula and B. K. Saha., *Cryst. Growth Des.*, 2015, **15**, 593.

335   15. S. J. James, A. Perrin, C. D. Jones, D. S. Yufit and J. W. Steed, *Chem. Commun.* 2014, **50**, 12851.

336   16. G. O. Lloyd, and J. W. Steed, *Chem. Commun.* 2014, **50**, 1426.

337   17. T. B. Hayes, A. Collins, M. Lee, M. Mendoza, N. Noriega, A. A. Stuart and A. Vonk, *Proc. Natl.*

338   *Acad. Sci. U.S.A.*, 2002, **99**, 5476.

339   18. J. J. Zhang, Y. C. Lu and H. Yang, *J. Agric. Food Chem.*, 2014, **62**, 9657.

340   19. A. Grube, D. Donaldson, T. Kiely, and L. Wu, Pesticides Industry Sales and Usage 2006 and 2007

341   Market Estimates, U.S. Environmental Protection Agency Washington, DC, USA, 2011, pp14.

342   20. C. R. D. Lancaster and H. Michel, *J. Mol. Biol.*, 1999, **286**, 883.

343   21. M. W. Walter, *Nat. Prod. Rep.*, 2002, **19**, 278.

344   22. Y. Wang, C. U. Pittman Jr and S. Saebo, *J. Org. Chem.*, 1993, **58**, 3085.

345   23. A. Quesada, M. A. Fontecha, M. V. López, J. N. Low and C. Glidewell, *Acta Cryst. C*, 2008, **64**, 463.

346   24. Bruker, SADABS, Bruker AXS Inc, 2001, Madison, Wisconsin, USA.

347   25. Bruker, APEX2 and SAINT, Bruker AXS Inc 2007, Madison, Wisconsin,USA.

348 26. G. Sheldrick, *Acta Cryst. A*, 2008, **64**, 112.

349 27. O. V. Dolomanov, L. J. Bourhis, R. J. Gildea, J. A. K. Howard and H. Puschmann, *J. Appl. Cryst.*,

350 2009, **42**, 339.

351 28. C. F. Macrae, I. J. Bruno, J. A. Chisholm, P. R. Edgington, P. McCabe, E. Pidcock, L. Rodriguez-

352 Monge, R. Taylor, J. van de Streek and P. A. Wood, *J. Appl. Cryst.*, 2008, **41**, 466-470.

353 29. W. Kabsch, *J. Appl. Cryst.*, 1993, **26**, 795.

354 30. Molinspiration Property Calculation Service (www.molinspiration.com).

355 31. M.-X. Wang, H.-B. Yang, *J. Am. Chem. Soc.*, 2004, **126**, 15412.

356 32. G. Kaupp, *Top. Curr. Chem.*, 2005, **254**, 95.

357 33. K. Tashiro, A. N. Zadorin, S. Saragai, T. Kamae, A. Matsumoto, K. Yokoi and S. Aoki,

358 *Macromolecules*, 1999, **32**, 7946.

359

The chloro-*s*-triazine herbicides, simazine and atrazine, assemble as hydrogen-bonded tapes in the solid state. The CCDC shows these tapes persisting across a wide range of *bis-N*-alkyl-chloro-*s*-triazines.